

Article

Nitrogen Doped Superactivated Carbons Prepared at Mild Conditions as Electrodes for Supercapacitors in Organic Electrolyte

María José Mostazo-López ¹, Ramiro Ruiz-Rosas ¹, Tomomi Tagaya ²,
Yoshikiyo Hatakeyama ², Soshi Shiraishi ², Emilia Morallón ³ and
Diego Cazorla-Amorós ^{1,*}

¹ Departamento de Química Inorgánica and Instituto Universitario de Materiales, Universidad de Alicante, Apartado 99, 03080-Alicante, Spain; mj.mostazo@ua.es (M.J.M.-L.); ramiro@ua.es (R.R.-R.)

² Division of Molecular Science, Graduate School of Science and Technology, Gunma University, Gunma 376-8515, Japan; t181a059@gunma-u.ac.jp (T.T.); y-htkym@gunma-u.ac.jp (Y.H.); soshishiraishi3@gunma-u.ac.jp (S.S.)

³ Departamento de Química Física and Instituto Universitario de Materiales, Universidad de Alicante, Apartado 99, 03080-Alicante, Spain; morallon@ua.es

* Correspondence: cazorla@ua.es

Received: 10 August 2020; Accepted: 17 September 2020; Published: 20 September 2020



Abstract: Nitrogen functionalization of a highly microporous activated carbon ($S_{\text{BET}} > 3000 \text{ m}^2/\text{g}$), to be used as electrode of electric double layer capacitor (EDLC), was carried out by different methods based on organic chemistry protocols at low temperature and selective thermal post-treatments under inert atmosphere. The combination of both methods allowed the production of carbon materials with very similar surface area (2400–3000 m^2/g) and different surface chemistry. The nitrogen functionalization by chemical methods produce the attachment of 4 at. % N (XPS) by consumption of oxygen functional groups. The thermal treatments rearrange the surface chemistry by decreasing and converting both nitrogen and oxygen moieties. The effect of surface chemistry on the performance of these materials as electrodes for symmetric supercapacitors was analyzed in organic electrolyte (1M TEMABF₄/propylene carbonate). The devices showed high gravimetric capacitance (37–40 F/g) and gravimetric energy density (31–37 Wh/kg). The electrochemical stability of the EDLC was evaluated by a floating test under severe conditions of voltage and temperature. The results evidence an improvement of the durability of nitrogen-doped activated carbons modified by chemical treatments due to the decrease of detrimental oxygen functionalities and the generation of nitrogen groups with higher electrochemical stability.

Keywords: electric double layer capacitor; porous carbon; nitrogen doping; surface chemistry

1. Introduction

Electrochemical capacitors (supercapacitors) are energy storage devices of great interest mainly due to their high power density, durability and broad operation temperature range [1,2]. However, it is necessary to increase their energy density for enabling their use in a wider range of applications. This requires the use of electrode materials and electrolytes able to increase both the capacitance and the operation voltage of electrochemical capacitors. Regarding the electrode materials, carbon materials are the most commonly used for the electric double layer capacitor (EDLC) as a carbon-based symmetric electrochemical capacitor since they have a well-developed porosity, electrochemical stability, and tunable surface chemistry [3,4]. In case of the electrolyte, the use of non-aqueous electrolytes (organic electrolytes and ionic liquids) has attracted great interest as consequence of their possible use at

high operation voltage [5,6]. The higher voltage charge realizes the higher energy density. Nonetheless, the use of excessively high operation voltage dramatically affects the performance of the electrodes, since carbon materials undergo reactions with the electrolyte that decrease their electrochemical stability, and consequently, diminish the cycle life of the device [7–9]. Hence, the development of carbon materials with improved electrochemical stability and durability is highly needed for their use in electrochemical capacitors.

The performance of carbon materials can be enhanced by different strategies [10]. One of the main approaches consists in synthesizing materials doped with different heteroatoms [11,12], such as sulfur, phosphorus or nitrogen, since they modify the electrochemical behavior of the material [7,13–16]. More specifically, nitrogen doping can increase the wettability, conductivity, and electrochemical stability [7,8,17–20]. However, the role of the different nitrogen groups is not still well understood. The isolation of selective functional groups on the surface of carbon materials is still a challenge since the formation of different functionalities depends on the temperature treatment and coexist with other surface groups. Moreover, the most common methods for producing nitrogen-doped carbon materials usually affect other key parameters on the performance of carbon electrodes: the porous structure and the oxygen functional groups [21,22]. Thus, understanding of the effect of nitrogen groups requires an ideal preservation of both oxygen functional groups and porous texture.

Nitrogen doped carbon materials can be prepared by several methods [23–27] that can be classified as follows: (i) by using a nitrogen-containing compound as additive or even as carbon source in different synthesis methods, such as carbonization (followed by activation) or templating methods; (ii) through post-treatments of a material previously synthesized with a nitrogen-containing reactant in gas or liquid phase. The latter methods usually involve the use of high temperatures to favor the incorporation of nitrogen, whether in gas or liquid phase. Moreover, the temperature treatment strongly affects the porosity of carbon material and produces other changes on the surface chemistry, such as the modification (via removal, attachment, or transformation) of oxygen functional groups. Thus, the attachment of nitrogen moieties while preserving other properties requires the use of less common methodologies. In this sense, the post-modification of the surface chemistry of carbon materials using strategies based on organic chemistry protocols is especially interesting, mainly because the incorporation of nitrogen is produced via consumption of oxygen groups and consequently the porous texture remains invariable. The modification of porosity is only a consequence of the amount and size of the nitrogen groups that have been incorporated. In this sense, we have developed nitrogen functionalization methods at mild conditions that allow the incorporation of a wide range of nitrogen functionalities while preserving the structure of the pristine carbon material, even when using carbon materials with extraordinary microporosity [9,28]. Moreover, the method also modifies porous carbon monolith, of which the interior is not easy to react with chemicals, such as seamless activated carbon electrodes [29]. These nitrogen-doped carbon materials can be used as a platform for producing selective nitrogen functional groups by heat treatments at selective temperatures under conditions that only the desorption of surface groups is produced, and consequently, the porosity remains invariable. Thus, an accurate selection of surface chemistry modification methods can be considered as an adequate strategy to produce highly microporous carbon materials with very similar porous texture and specific functional groups.

The aim of this work is to elucidate the role of different nitrogen functionalities on the performance of activated carbons as electrodes for the EDLC using organic electrolyte, mainly focusing on their effect on the electrochemical stability and durability of the device. We propose the synthesis of nitrogen-doped activated carbons with high apparent surface area by combining functionalization methods based on wet methods at low temperatures and post-thermal treatments at different temperatures, whose combination allows a selective modification of the surface chemistry. The effect of different nitrogen functionalities and doping methods on the performance of these materials as electrodes for the EDLC is tested in typical organic electrolyte and severe conditions of temperature and operation voltage.

2. Materials and Methods

2.1. Synthesis of Carbon Materials

2.1.1. Pristine Carbon Material

An activated carbon with high microporosity prepared in our laboratory has been used as the starting material for nitrogen incorporation via post-modification treatments. The pristine material (named as KUA) has been synthesized by chemical activation of a Spanish anthracite with KOH (CAS number: 1310–58–3, 85%, AnalaR Normapur, VWR Chemicals, USA) using an impregnation ratio of activating agent to raw material of 4:1 and an activation temperature of 750 °C under inert atmosphere, which was held for 1 h. More details about the preparation process are available elsewhere [30].

2.1.2. N-Functionalization of Carbon Materials at Mild Conditions

KUA was further functionalized with nitrogen functional groups by two different approaches based on the organic chemistry reactions described in refs. [9,28]. The first approach consisted in a three-step protocol combining oxidation and amidation reactions, that is described as follows:

- (i) Oxidation treatment. 1 g of activated carbon (KUA) was mixed with 40 mL of HNO₃ 65 wt % under stirring during 3 h at room temperature. After that, the activated carbon was filtrated and washed with Milli-Q water until the pH of elution was neutral. Finally, the sample (named KUA-COOH) was dried at 100 °C.
- (ii) Treatment with SOCl₂. 1 g of KUA-COOH was introduced in a round bottom flask with 50 mL of toluene and 5 mL of SOCl₂ (CAS number: 7719–09–7, 97%, Sigma-Aldrich, Saint Louis, MO, USA) was added to the flask. The mixture was refluxed at 120 °C for 5 h and finally washed with toluene and dried for 14 h.
- (iii) The activated carbon obtained in step (iii) was added into a 2M NH₄NO₃ diluted in N,N-dymethylformamide (CAS number: 68–12–2, Sigma-Aldrich, EEUU) in a round bottom flask, using an activated carbon to solution ratio of 1 g/150 mL. Then, 150 mL of pyridine (CAS number: 110–86–1, 99%, Acros Organics, Fisher Scientific, Waltham, MA, USA) were added slowly to the round bottom flask under continuous stirring at room temperature. The mixture was stirred at 70 °C for 65 h. The obtained amidated sample (KUA-CONH₂) was washed with abundant water and ethanol, filtered, and dried at 100 °C overnight.

In the second approach, the amidation reaction (third step of the first method) is directly applied over pristine sample (KUA). This sample was named as KUA-N. More details about the preparation methods are found elsewhere [9,28].

2.1.3. Heat Treatments

The carbon materials (KUA, KUA-CONH₂ and KUA-N samples) were heat treated at two different temperatures for 1 h under N₂ atmosphere using a flow of 200 mL/min and a heating rate of 5 °C/min. The obtained samples were labelled as KUA_n, KUA-CONH₂_n and KUA-N_n, where n is the final heating temperature (500 and 800 °C).

2.2. Physicochemical Characterization

The surface chemistry of the samples was analyzed by X-ray photoelectron spectroscopy (XPS) and temperature programmed desorption (TPD). XPS analyses were performed using a VG-Microtech Multilab 3000 spectrometer with an Al anode. N1s spectra were deconvoluted using Gaussian functions with 20% of Lorentzian component. A Shirley line was used as background and the FWHM of the peaks was kept between 1.4 and 1.7 eV. The experimental error is ± 0.2 eV. TPD experiments were carried out using a TGA-DSC instrument (TA Instruments, SDT Q600 Simultaneous) coupled to a mass spectrometer (Thermostar, Balzers, BSC 200, Asslar, Germany), by heating the samples up to 950 °C

(heating rate: 20 °C/min) under helium atmosphere (flow rate: 100 mL/min). The experimental error in this technique is $\pm 10 \mu\text{mol/g}$.

The porous texture characterization was carried out by N₂ adsorption-desorption isotherms at $-196 \text{ }^\circ\text{C}$ and by CO₂ adsorption at 0 °C using an Autosorb-6-Quantachrome apparatus. The samples were outgassed at 200 °C for 4 h before the experiments. The apparent surface area was obtained from N₂ adsorption isotherms by using the BET equation in the 0.05–0.20 range of relative pressures. The total micropore volume was determined by Dubinin–Radushkevich (DR) method applied to N₂ (relative pressures from 0.01 to 0.05) adsorption isotherms. The volume of the narrow microporosity (i.e., pore sizes below 0.7 nm) was calculated from the DR method applied to the CO₂ adsorption isotherms (relative pressures from 0.0001 to 0.20) [31]. The experimental errors are $\pm 0.01 \text{ cm}^3/\text{g}$ for micropore volume (V_{DR}) and $\pm 10 \text{ m}^2/\text{g}$ for apparent surface area (S_{BET}), also taking into account the reproducibility of the measurement.

2.3. Electrochemical Characterization

The carbon materials were used for the preparation of the electrodes for two-electrode sealed cells (Al/Mg-body flat cell, Hohsen Corporation, Osaka, Japan). The electrodes were prepared by mixing the carbon material with acetylene black and polytetrafluoroethylene (PTFE) in a ratio of 85:10:5 wt %. The electrodes were pressed to shape disks with a diameter of 13 mm and a thickness of $\sim 0.5 \text{ mm}$ (net weight: 35 mg). Etched aluminium foil (20C054, Japan Capacitor Industrial Co., Ltd., Tokyo, Japan) as current collector was attached to the electrode by using conductive carbon paste (GA-715, Hitachi Chemical Co., Ltd., Tokyo, Japan). Cellulose fiber paper was used as separator and 1M triethylmethylammonium tetrafluoroborate diluted in propylene carbonate (TEMA-BF₄/PC, Toyo Gosei Co., Ltd., Tokyo, Japan) as electrolyte. The cells were assembled with the two identical electrodes as positive and negative electrode, the separator, and the electrolyte inside an Argon glovebox.

All electrochemical characterization was conducted using charge-discharge system (HJ-1001SM8, Hokuto Denko Co., Tokyo, Japan). The cells were tested by galvanostatic charge-discharge (GCD) cycles between 0–2.5 V with different current densities (40, 100, 200, 400, 600, 1000 mA/g) at 40 °C. These current densities were determined by normalizing the actual current value with the total active mass of the carbon in both of the positive and negative electrodes in the full cell. The capacitance was calculated from the discharge curve of the GCD cycles as reported previously in the literature [32]. The capacitance values are given with an experimental error of $\pm 1 \text{ F/g}$. The gravimetric capacitance is referred to the total active mass of the carbon in the cell in the same manner as the current density. Afterwards, a durability test (based on GCD cycles and floating test) was performed by applying the following procedure: (i) 5 GCD cycles at 2.5 V and 40 °C; (ii) 5 GCD cycles at 2.5 V and 70 °C; (iii) 5 GCD cycles at 3.2 V and 70 °C; (iv) voltage is kept at 3.2 V for 100 h (floating test). After finishing the floating test (iv), steps (iii), (ii) and (i) were subsequently repeated. The capacitance, internal resistance and integrated leakage current were calculated. The retention of capacitance is given at 2.5 V and 40 °C. The current density was kept as 40 mA/g during the experiment.

3. Results and Discussion

3.1. Physicochemical Characterization of Carbon Materials

3.1.1. Porous Texture

Figure 1 illustrates the N₂ adsorption-desorption isotherms obtained for all activated carbons. The profiles evidence that all carbon materials show an adsorption-desorption curve characteristic of microporous materials. Table 1 summarizes the porous texture parameters obtained from N₂ and CO₂ isotherms for all the activated carbons; the pristine sample KUA, the treated at 800 °C (KUA_800) and the oxidized in nitric acid (KUA-COOH) have been included for comparison purposes. The changes in the porous texture of the samples obtained by oxidation (KUA-COOH) and chemical

functionalization (KUA-CONH₂ and KUA-N) were previously discussed [9,28]. The most significant change is observed for KUA-COOH and KUA-CONH₂ samples, as consequence of the generation of oxygen functionalities in KUA-COOH and their conversion into nitrogen functional groups that occupy or block part of the microporosity [28] (Table 1, Figure 2b,c). However, when the chemical method is directly applied over the pristine sample (sample KUA-N), the microporosity of the material is fully preserved (as demonstrated in Figure 1a, Table 1).

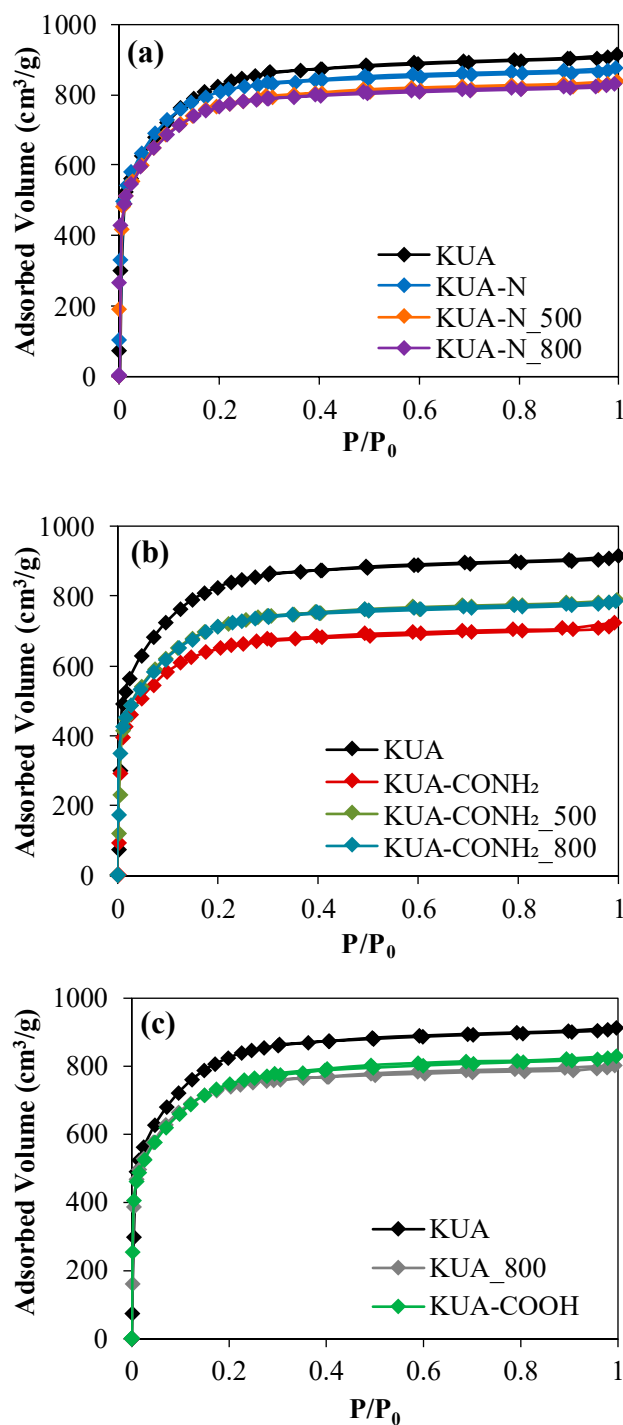
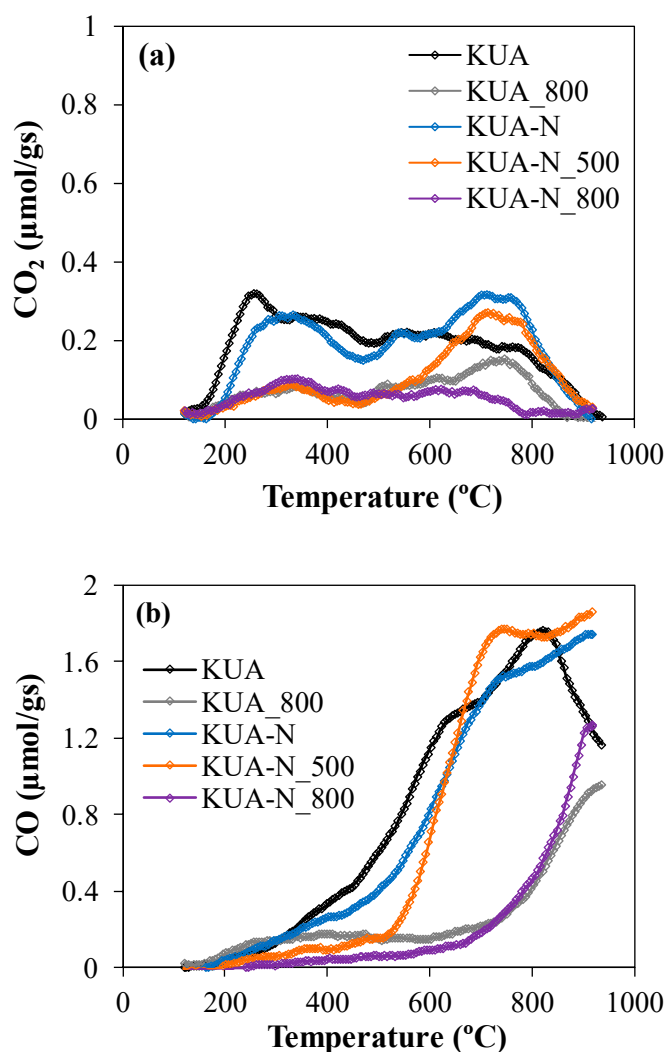


Figure 1. N₂ adsorption-desorption isotherms obtained for all activated carbons: (a) KUA, KUA-N and related heat-treated samples, (b) KUA, KUA-CONH₂ and related heat-treated samples, (c) KUA and related heat-treated sample.

Table 1. Porous texture of the activated carbons.

Sample	S_{BET} (m^2/g)	$V_{\text{DR}}^{\text{N}_2}$ (cm^3/g)	$V_{\text{DR}}^{\text{CO}_2}$ (cm^3/g)
KUA	3080	1.19	0.57
KUA_800	2720	1.05	0.49
KUA-N	2960	1.18	0.52
KUA-N_500	2800	1.11	0.49
KUA-N_800	2770	1.09	0.48
KUA-COOH	2770	1.06	0.49
KUA-CONH ₂	2390	0.97	0.45
KUA-CONH ₂ _500	2630	1.02	0.41
KUA-CONH ₂ _800	2630	1.0	0.43

**Figure 2.** Comparison between (a) CO₂ and (b) CO TPD profiles of KUA, KUA_800, KUA-N, KUA-N_500 and KUA-N_800.

Regarding the heat-treated samples, some loss of the microporosity is detected when the heat treatment is carried out over KUA and KUA-N samples (Figure 1a,c, Table 1). This change could be produced by some structural rearrangement in the materials [33]. However, the heat treatments over KUA-CONH₂ produce an increase of the micropore volume (see samples KUA-CONH₂_500 and KUA-CONH₂_800). This increase of microporosity is related to the removal of functional groups that occupy or block part of the microporosity in the pristine sample. Interestingly, the thermal treatments at different temperatures (500 °C and 800 °C) produce identical modifications on the

porous texture of the pristine sample (KUA-N and KUA-CONH₂). As consequence, the N₂ adsorption isotherms obtained for samples KUA-N_500 and KUA-N_800 overlaps (Figure 1a). The same effect is observed for KUA-CONH₂_500 and KUA-CONH₂_800 samples (Figure 1b). The identical textural properties produced by the heat treatments at different temperatures indicate that the main textural rearrangements are produced at temperatures below 500 °C at the range of temperatures used.

The CO₂ micropore volumes (collected in Table 1) provide information about the narrow microporosity of the samples (<0.7 nm) [31]. It is observed that the chemical functionalization and the heat treatments produce a small decrease of the narrow microporosity. The largest micropore volume was found for the pristine sample KUA, followed by the KUA-N activated carbon and its related heat-treated samples (KUA-N_500 and KUA-N_800).

The pore size distribution was analyzed and is shown in the Supplementary Data (Figure S1). The pristine carbon material displays a wide pore size distribution and an average pore size of 1.4 nm. The surface modification methods do not produce significant changes in the pore size distribution of the functionalized carbons. The profiles show that the modification treatments mainly affect the largest micropores (>1 nm), while the narrowest micropores remain almost invariable. However, KUA-N activated carbon (and its related heat treated samples) experience an increase of the amount of micropores below 1 nm, indicating that the functionalization method produces the occupation of the largest micropores and, in consequence, decreases their size.

3.1.2. Surface Chemistry Characterization

The surface chemistry of the activated carbons was characterized by XPS and TPD. Table 2 collects the data related to the chemical composition of the samples. Figures 2 and 3 collect the TPD profiles obtained for all activated carbons. The pristine carbon material KUA possesses a large amount of oxygen functionalities that decompose mainly as CO and in lower extent as CO₂ (Figure 2). The chemical modification methods produce the attachment of nitrogen to the surface of the pristine activated carbon by consumption of oxygen functional groups, as confirmed by XPS (Table 2). Figure 4 shows the deconvoluted N1s spectra obtained for all N-doped activated carbons and Table 3 summarizes the relative amount of the detected N functional groups. In case of KUA-N sample, the attachment of nitrogen occurs directly over the pristine carbon material via reaction mainly with CO-evolving groups. Thus, this treatment produces nitrogen groups derived from these oxygen functionalities, such as imines, amines and N heterocycles (pyrroles, pyridones, and pyridines) [25,34–36] (Figure 2a). In the case of the KUA-CONH₂ sample, an oxidation treatment is carried out, previously to the incorporation of nitrogen, to increase the amount of oxygen functional groups that can react during the amidation treatment. The oxidation treatment with HNO₃ produces an increase of both CO and CO₂ evolving-groups, and consequently the nitrogen moieties produced after the nitrogen doping treatment are mainly in form of amides (and cyclic amides), pyridines, and pyrroles/pyridones [25,34–36]. Hence, both N-doped carbons obtained at mild conditions evidence the presence of different N functional groups, being KUA-CONH₂ richer in those derived from CO₂-evolving groups (amides, lactams, and imides).

Table 2. Surface composition of the activated carbons obtained by XPS and TPD.

Sample	CO ₂ TPD (μmol/g)	CO TPD (μmol/g)	O TPD (μmol/g)	O _{XPS} (at. %)	N _{XPS} (at. %)
KUA	450	1970	2870	8.8	0.3
KUA_800	170	620	960	2.3	
KUA-N	450	1750	2640	7.5	3.7
KUA-N_500	250	1620	2120	5.1	2.3
KUA-N_800	130	505	720	3.0	1.7
KUA-COOH	1790	3770	7360	15.8	
KUA-CONH ₂	1140	2370	4650	10.2	4.2
KUA-CONH ₂ _500	250	1650	2140	8.0	3.4
KUA-CONH ₂ _800	140	570	830	4.5	2.1

The surface chemistry of the carbon materials was subsequently modified by heat treatments under inert atmosphere to produce activated carbons with different composition while keeping unmodified the porous texture of the pristine materials. These treatments produce a decrease of oxygen and nitrogen groups (Table 2). TPD profiles allow to get information about the changes produced in the oxygen functionalities (Figures 2 and 3). When the treatment at 500 °C is carried out, some oxygen functionalities are removed from their surface; the main loss comes from CO₂-evolving groups, since most part of these functionalities are not thermally stable at temperatures higher than 600 °C [37]. Thus, no significant changes are produced on KUA-N at this temperature, as a result of the small number of CO₂-evolving groups in this sample. Consequently, KUA-N₅₀₀ shows a similar composition as that of KUA-N, with slightly lower oxygen content. More important differences are found for KUA-CONH₂₅₀₀ due to the larger amount of oxygen (specially, CO₂-evolving groups) of the parent carbon (KUA-CONH₂). After the treatment, most of the CO₂ groups are removed from this sample (80% decrease, Table 2). Moreover, an important decrease of the CO-evolving groups is also observed (30% decrease, Table 2). Interestingly, both carbons heat-treated at 500 °C show almost identical content of oxygen groups (measured by TPD, Table 2, Figures 2 and 3). The oxygen content reported by XPS displays different values since this technique measures the atomic composition in the outer part of the carbon particles, while TPD provides the amount of CO₂ and CO evolving groups produced by the desorption of oxygen functionalities in the inner and the outer regions of the carbon particles.

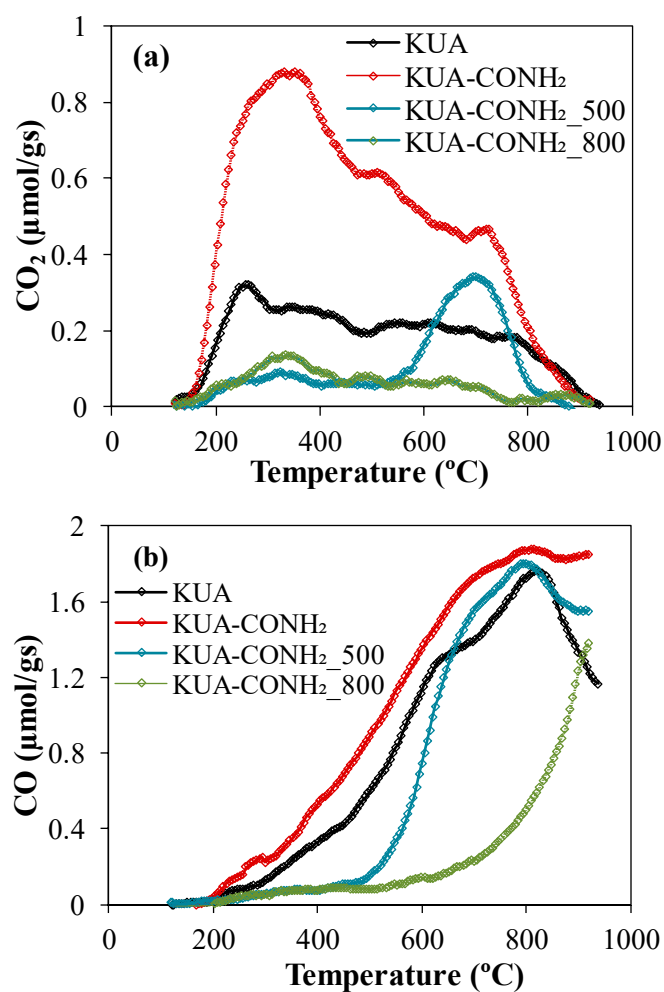


Figure 3. Comparison between (a) CO₂ and (b) CO TPD profiles of KUA, KUA-CONH₂, KUA-CONH₂₅₀₀ and KUA-CONH₂₈₀₀.

The heat treatment at 800 °C removes most of oxygen. Around 70–80% of oxygen functionalities are removed from KUA, KUA-N, and KUA-CONH₂ when they are heat treated at 800 °C. N functionalities also decrease upon heat treatment and around 50% of N remains after the treatment. Hence, the obtained samples show similar oxygen contents (mainly in form of carbonyles [37]) and an almost identical porous texture (Section 3.1.1.).

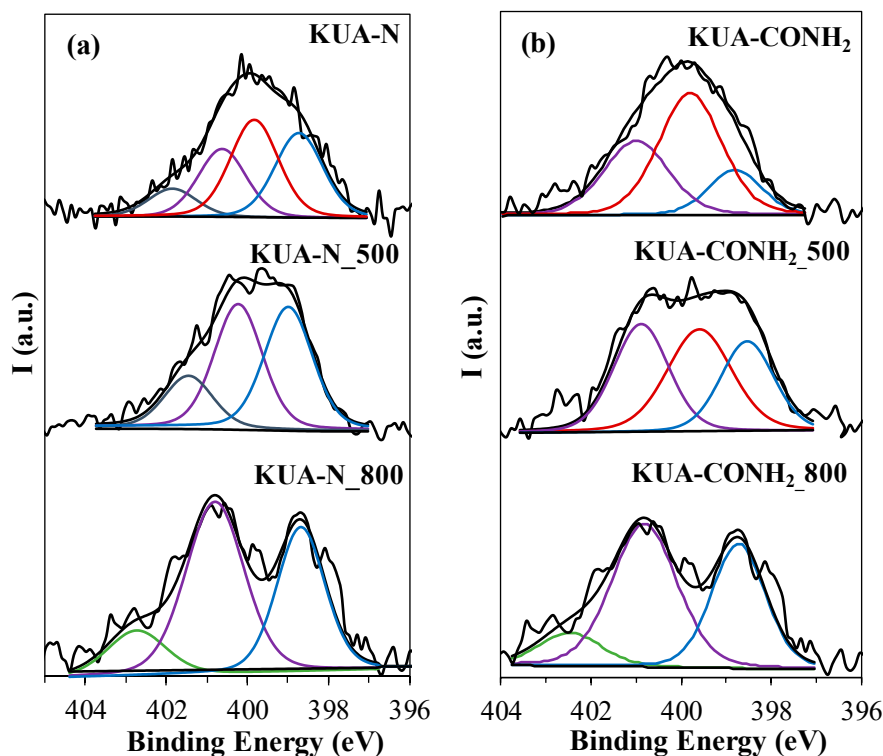


Figure 4. N1s XPS spectra deconvoluted for (a) KUA-N, KUA-N₅₀₀ and KUA-N₈₀₀ activated carbons and (b) KUA-CONH₂, KUA-CONH_{2_500} and KUA-CONH_{2_800} activated carbons.

The deconvolution of N1s XPS spectra obtained for all N-doped activated carbons allows to assess the modifications produced on the nitrogen moieties during the thermal treatments (Figure 4). Table 3 collects the ratio of each nitrogen group obtained from the N1s XPS spectra. As previously described, the N-doped carbons at mild conditions (KUA-N and KUA-CONH₂) have similar nitrogen contents but, according to the modification pathway, some of the generated groups are different. The peak at 399.8 ± 0.2 eV can be assigned to amides (and cyclic amides) and amines, being more likely the formation of amides in KUA-CONH₂ (due to the previous oxidation process) and amines in KUA-N [18].

When the samples are heat treated at 500 °C, the nitrogen moieties of lower thermal stability are removed, i.e., those with a single chemical bond, such as amines and amides [38]. Indeed, the heat treatment of KUA-N produces a loss of 1.4 at. % N (Table 2), that is in agreement with the amount of amines detected in KUA-N, and that does not appear in the spectrum of KUA-N₅₀₀ (Figure 4a), evidencing the preferential removal of this functional group during the treatment. In case of KUA-CONH₂, a lower loss of nitrogen is detected (0.8 at. % XPS, Table 2). Likewise, the main decrease is associated to the functional groups at 399.8 ± 0.2 eV, i.e., amide-like functionalities (Table 3, Figure 4b), but they are still detected on KUA-CONH_{2_500}. Moreover, this sample evidences an increase of pyrrole/pyridones contribution (400.7 ± 0.2 eV) that can be related to the rearrangements of amides to generate pyrroles upon heating [35], explaining the higher retention of nitrogen in this sample.

Table 3. Assignment of N1s deconvoluted curves to nitrogen functional groups.

Sample	Binding Energy (eV)	Functional Group	N (at. %)	Ratio of N Species (%)
KUA-N	401.9 ± 0.2	Quaternary	0.4	10
	400.7 ± 0.2	Pyrrole, Pyridone	0.9	25
	399.8 ± 0.2	Amide, Lactam, Amine, Imide	1.3	35
	398.7 ± 0.2	Pyridine, Imine	1.1	30
KUA-N_500	401.5 ± 0.2	Quaternary	0.4	17
	400.2 ± 0.2	Pyrrole, pyridone	0.9	42
	399.0 ± 0.2	Pyridine, Imine	1.0	41
	402.7 ± 0.2	Oxidized N	0.3	14
KUA-N_800	400.8 ± 0.2	Pyrrole, Pyridone	1.2	51
	398.7 ± 0.2	Pyridine	0.8	35
	400.7 ± 0.2	Pyrrole, pyridone	0.7	19
KUA-CONH ₂	399.8 ± 0.2	Amide, lactam, amine, imide	1.9	50
	398.8 ± 0.2	Pyridine, imine	1.2	31
	400.9 ± 0.2	Pyrrole, pyridone	1.7	34
KUA-CONH ₂ _500	399.6 ± 0.2	Amide, lactam, amine, imide	1.3	38
	398.5 ± 0.2	Pyridine, imine	1.0	28
	402.5 ± 0.2	Oxidized N	0.2	11
KUA-CONH ₂ _800	400.8 ± 0.2	Pyrrole, pyridone	0.9	52
	398.7 ± 0.2	Pyridine, imine	0.6	37

The heat treatments at 800 °C strongly decrease the nitrogen groups of the N-doped samples (Table 2, Figure 4). The samples KUA-N_800 and KUA-CONH₂_800 show similar nitrogen content (1.7 at. % and 2.1 at. %, respectively, Table 2) and distribution of functionalities, with a main contribution of pyrroles/pyridones and a lower presence of pyridines and quaternary nitrogen (Table 3). These modifications are undoubtedly related to the removal of nitrogen groups of lower thermal stability as well as their conversion into more stable groups, such as nitrogen heterocycles [35].

Thus, the combination of nitrogen doping at mild conditions with post-thermal treatments allow the production of activated carbon with similar microporosity and different surface functionalities. Hence, their electrochemical characterization in organic electrolyte can be useful to get information about the role of the different N functional groups in the electrochemical performance of the materials as electrodes for supercapacitors.

3.2. Electrochemical Characterization

The electrochemical performance of the samples was evaluated as electrodes in the EDLC (activated carbon-based symmetric electrochemical capacitors) with organic electrolyte (1M TEMABF₄/PC) by using a two-electrode cell configuration. The cells were tested by GCD cycles at different current densities. Table 4 collects the capacitance and energy obtained from the galvanostatic test and Figure 5 shows, as an example, some of the charge-discharge curves obtained for the capacitors at 40 mA/g. The curves evidence an ideal capacitive behaviour, characterized by the triangular shape, for all the activated carbon-based capacitors. All of them provide large capacitance (36–41 F/g) and gravimetric energy density (32–37 Wh/kg) as consequence of their well-developed microporosity. The small differences found between the samples are related to their slightly different apparent surface area, as confirmed by the similar surface capacitance values (specific capacitance per surface area) obtained for these materials (13–15 μF/cm²). The nitrogen doping does not produce an increase of capacitance as observed in other N-doped carbons [7,18] since the large microporosity development of these materials might mitigate this effect. Interestingly, the lowest values were obtained for the non-doped samples with a higher oxygen content (KUA and KUA-COOH), evidencing a detrimental effect derived from these functional groups [21].

Table 4. Gravimetric capacitance, surface capacitance, energy density, retention of capacitance at 1000 mA/g (C_1/C_0), retention of capacitance after floating test (C_f/C_0), increase of resistance and integrated leakage current obtained for all EDLCs. $V = 2.5$ V. $j = 40$ mA/g.

Capacitor	C_0 (F/g)	C_0/S_{BET} ($\mu\text{F}/\text{cm}^2$)	E (Wh/kg)	C_1/C_0 (%)	C_f/C_0 (%)	ΔR (Ω)	I_L (mAh)
KUA	41	13	37	45	29	33	37
KUA_800	38	14	33	48	43	30	29
KUA-N	41	14	36	42	39	20	32
KUA-N_500	41	15	35	45	39	32	36
KUA-N_800	40	14	35	49	44	28	31
KUA-COOH	36	13	31	30	20	50	26
KUA-CONH ₂	37	15	32	49	55	13	22
KUA-CONH ₂ _500	39	15	33	37	22	86	33
KUA-CONH ₂ _800	38	15	32	42	33	34	41

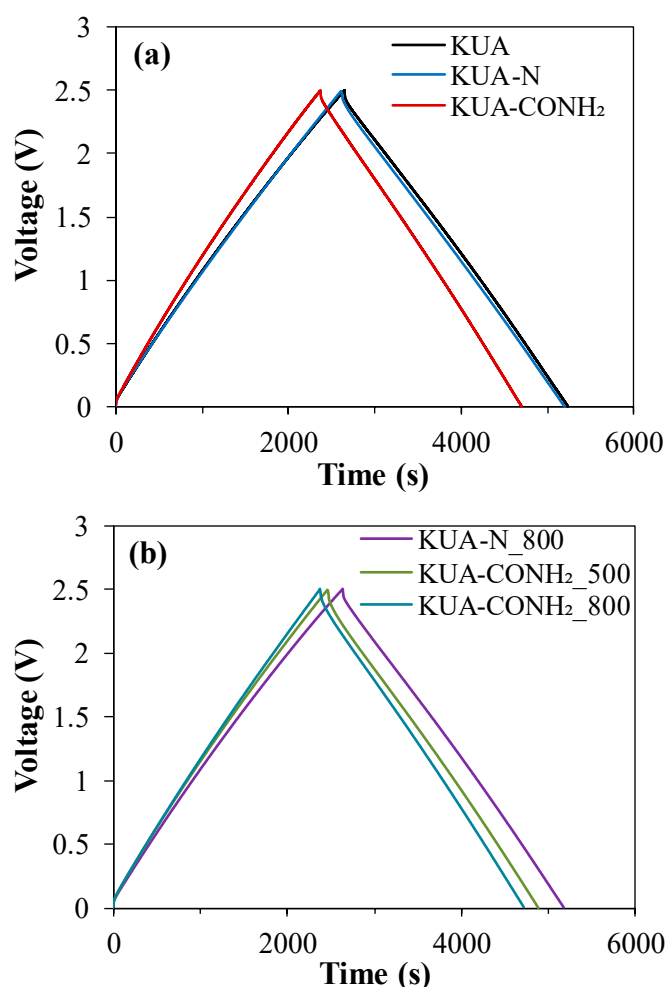


Figure 5. GCD curves obtained for selected EDLCs (activated carbons-based symmetric capacitors): (a) KUA, KUA-N and KUA-CONH₂ based capacitors; (b) KUA-N_800, KUA-CONH₂_500 and KUA-CONH₂_800. 1M TEMABF₄/PC. $j = 40$ mA/g. $V = 2.5$ V.

Figure 6 shows the evolution of the capacitance when increasing the current density during the galvanostatic cycling test. The GCD cycles recorded at high current density are shown in Figure S2 in the Supplementary Data. The oxidation process produces a detrimental effect on the rate performance of KUA-COOH when used as electrode for supercapacitors. Moreover, when the amidation treatment is carried out, the replacement of oxygen groups by nitrogen functionalities with a higher conductivity (cyclic amides, pyrroles, etc.) [18,39] improves the behaviour, and consequently, a higher capacitance is retained when the current density is increased (Figure 6a, Table 4, column C_1/C_0). The same trend

was observed in aqueous electrolyte [28]. The heat treatments of the activated carbons, which remove oxygen functionalities, produce an improvement of the rate performance, but the benefits by the heat-treatment is not significant for the N-doped samples (Figure 6b, Table 4, column C_1/C_0). Hence, the increase of the charge-discharge rate is mainly a consequence of an increase of conductivity due to the removal of electron-withdrawing oxygen functionalities.

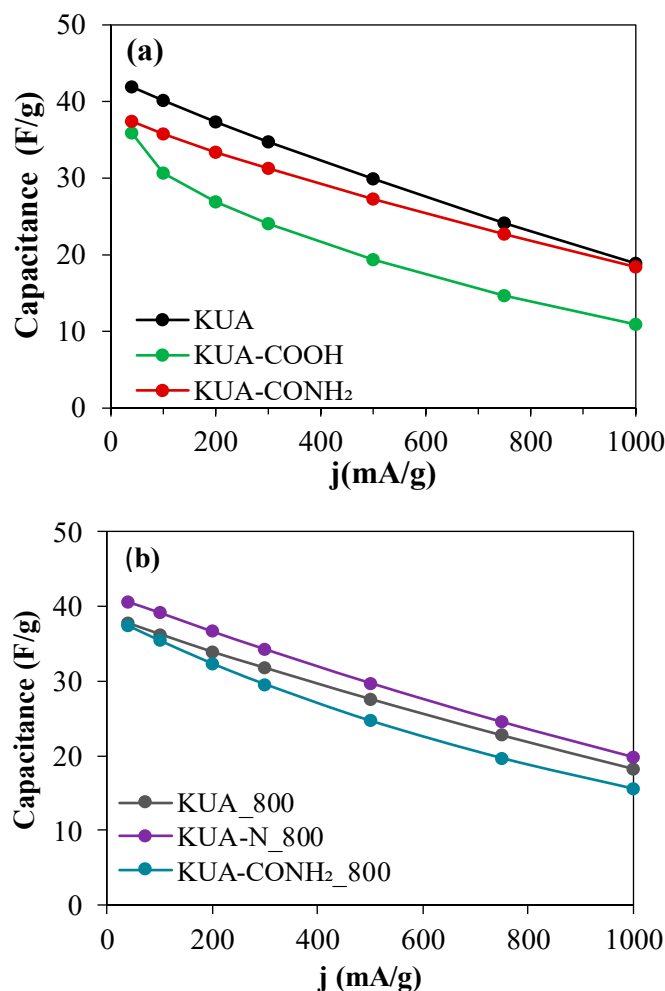


Figure 6. Rate performance (dependence of gravimetric capacitance on current densities) for selected EDLCs: (a) KUA, KUA-COOH and KUA-CONH₂; (b) KUA_800, KUA-N_800 and KUA-CONH₂_800. 1M TEMABF₄/PC. $j = 40, 100, 200, 500, 750$ and 1000 mA/g. $V = 2.5$ V.

The EDLCs were submitted to a durability test to assess the effect of surface chemistry in the electrochemical stability of the carbon materials. The most common method for the assessment of the durability of energy storage devices consists in applying thousands of GCD cycles at the operative voltage of the devices [10]. Since capacitors are based in electrostatic processes and consequently provide a much larger cycle life than batteries, this methodology is considerably more time demanding for supercapacitors [1]. An alternative to this procedure is the use of a floating test, consisting in keeping the cell charged during long time in order to accelerate the degradation of the device [40–44]. Moreover, it is well-known that electrochemical capacitors experience degradation at high temperature [6,21,45,46]. Hence, the combination of high voltage holding with the use of high temperature constitutes an adequate procedure to accelerate the degradation of electrochemical capacitors.

Figure 7 shows, as an example, the evolution of capacitance and coulombic efficiency during the steps of the durability test (described in Section 2.3.) for some of the capacitors. Table 4 compiles the parameters (retention of capacitance (C_f/C_0), increase of resistance (ΔR) and integrated leakage current

(I_L) related to this test determined for all capacitors. The analysis of these data allows for a thorough discussion of the effect of surface chemistry modification on the performance of carbon materials as electrodes for supercapacitors in organic electrolyte.

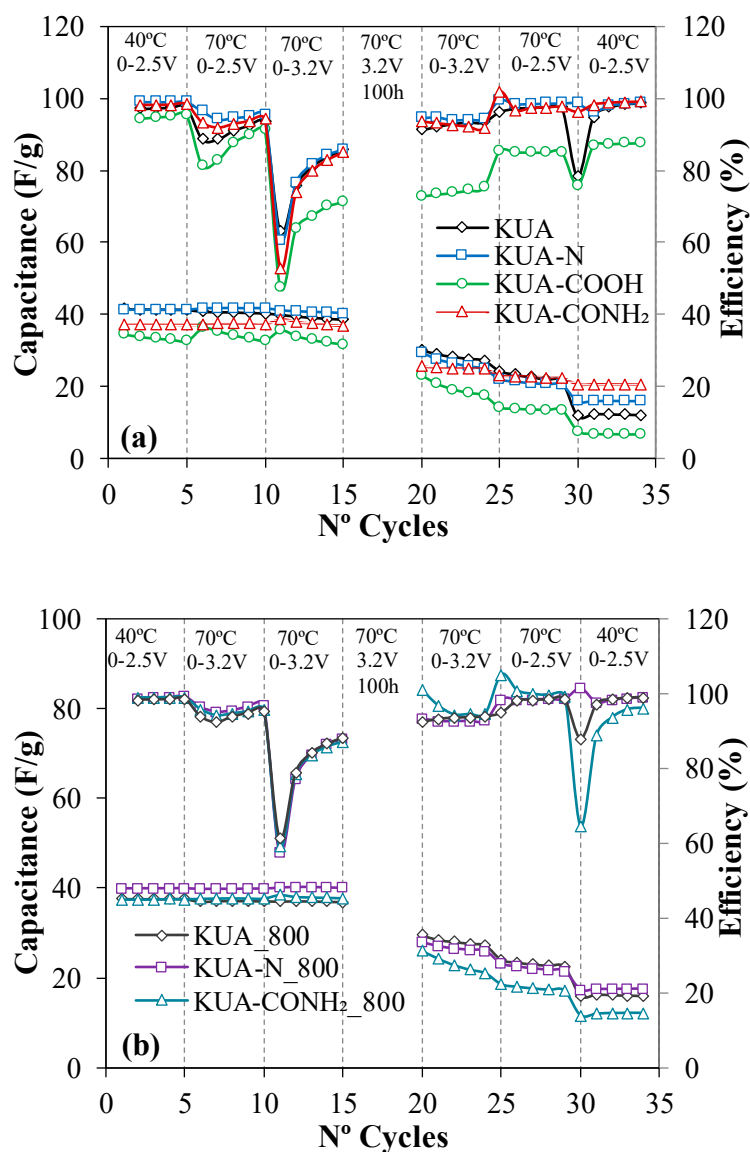


Figure 7. Evolution of capacitance and coulombic efficiency during the durability test for selected EDLCs: (a) KUA, KUA-N, KUA-COOH and KUA-CONH₂; (b) KUA₈₀₀, KUA-N₈₀₀ and KUA-CONH₂₈₀₀. 1M TEMABF₄/PC. $j = 40$ mA/g.

3.2.1. Effect of Surface Chemistry Modification at Mild Conditions

Figure 7a displays the performance of the pristine carbon material during the durability test. The test starts with a conventional galvanostatic cycling step at 40 °C and 2.5 V, followed by two steps at increased temperature (70 °C) and loading voltage (3.2 V and 70 °C) conditions. Such increases do not affect the gravimetric capacitance, but they have a negative impact on the coulombic efficiency evidencing the occurrence of faradaic processes under these conditions. After these steps, a floating test of 100 h takes part at rather severe conditions (3.2 V and 70 °C). The harmful effect of the floating conditions is clearly observed in the capacitance values determined after the durability test. For the pristine sample, only a 29% of capacitance is retained after the ageing test.

In general, the N-doped samples show a similar trend for the durability to the pristine samples. Thus, a remarkable loss of capacitance (50–70%) is detected after the floating test for all supercapacitors (Table 4). The differences in the performance are a consequence of their different surface chemistry. First, it is confirmed that the oxidation process strongly affects the behavior of the capacitor, since a retention of capacitance of 20% and an increase of resistance of 50 Ω is detected for KUA-COOH based capacitor. Thus, the ageing protocol produces an enormous degradation of the electrodes due to reaction between the electrolyte and the oxygen groups present on the surface of the electrodes [21]. Otherwise, the N-doping treatments at mild conditions improve the performance of the carbon materials. Especially, KUA-CONH₂ based capacitor shows the best performance of all tested cells (Table 4). The retention of capacitance obtained is 55%, which means an increase of 26% in comparison with the pristine carbon-based capacitor (KUA). Moreover, the KUA-CONH₂ based capacitor shows the lowest integrated leakage current, which is associated to the occurrence of undesired faradaic reactions during the charging of the device (oxidation, gasification, etc.) [7,44]. As discussed in Section 3.1.2., KUA-CONH₂ shows predominance of amide-like functional groups as well as a lower amount of nitrogen heterocycles (pyridines and pyrroles/pyridones). Also, the sample has a larger content of oxygen functional groups than the pristine sample as consequence of the oxidation process carried out prior to the amidation. However, the increase in stability cannot be related to the oxygen functionalities since they damage the electrochemical stability, as evidenced by KUA-COOH based capacitor. Actually, the capacitance retention detected for KUA-CONH₂ is even higher (36%) when compared to the former oxidized sample KUA-COOH. Thus, the improvement of the performance is undoubtedly related to the generation of stable nitrogen surface functional groups.

Furthermore, KUA-N based capacitor also has better performance than the pristine carbon-based capacitor (Figure 7a, Table 4), evidencing an increase of capacitance retention of 11%. Since this sample is synthesized by a direct replacement of oxygen groups by nitrogen functionalities of KUA, the improvement might be a result of the combined effect caused by the removal of detrimental oxygen groups and generation of nitrogen moieties with higher electrochemical stability (pyrroles, pyridines, etc.). Moreover, the comparison of the N-doped samples (KUA-N and KUA-CONH₂) allows to distinguish the effect of the different nitrogen functional groups and evidence a remarkable stabilizing effect related to amides and cyclic amides, since these functional groups exist with the highest amount on the surface of KUA-CONH₂ and the corresponding capacitor shows a higher retention of capacitance and a lower increase of resistance than KUA-N based capacitor. This result can be considered as unusual since amide functional groups shows lower thermal stability than other nitrogen functionalities [35]. However, their cyclic forms (such as lactams) show larger thermal stability due to the incorporation of N heterocycles at the edge of the carbon layer. Moreover, they are tautomeric forms of pyridones, which provide larger thermal stability [28]. Although thermal and electrochemical stability might not be intrinsically related, these facts can help to clarify the improved performance showed by amide-functionalized activated carbon electrodes.

In order to deepen into the role of the different functionalities, the effect of heat treatments on the performance of activated carbons as electrodes for supercapacitors is thoroughly discussed.

3.2.2. Effect of Surface Chemistry Modification by Heat Treatments

The durability of the capacitors built with the heat-treated samples was also analyzed (Figure 7b) and the related parameters are collected in Table 4. Some meaningful differences are found when comparing the capacitor performance of the samples heat treated at 500 °C. KUA-N₅₀₀ based capacitor has better performance than the pristine carbon material KUA, as denoted by an increase of retention of capacitance of 10%. This sample has a similar surface chemistry to the parent KUA-N, with slightly lower content of oxygen and nitrogen groups (Section 3.1.2.). Thus, the improvement is related, again, to the removal of detrimental oxygen functional groups as well as the generation of more stable nitrogen groups. Nevertheless, the analogous KUA-CONH₂₅₀₀ based capacitor shows lower stability through the durability test (22% of capacitance retention, Table 4) than the

related carbon-based capacitors. Interestingly, the heat-treated N-doped carbons (KUA-CONH₂_500 and KUA-N_500) show different behavior upon durability even though their surface chemistry is almost identical in terms of amount of oxygen and nitrogen heteroatoms (Section 3.1.2). The main difference arises from their parent carbons (KUA-CONH₂ and KUA-N). KUA-CONH₂ has a larger amount of surface functionalities, that upon heating may decompose and generate a larger number of reactive sites. Consequently, the capacitor based on the activated carbon prepared by the heat treatment of KUA-CONH₂ might experience more interactions with the electrolyte, leading to a higher degradation process.

The heat treatment of the samples at 800 °C also affect the durability of the devices. It is clearly observed that the treatment under these conditions improve the performance as consequence of the high decrease of oxygen functionalities. Thus, KUA_800 and KUA-N_800 have a similar behavior upon the floating test, with an increase of retention of capacitance of ~14% for both capacitors (in comparison with KUA-based capacitor). Hence, no further improvement results from the nitrogen groups present on KUA-N_800. In case of KUA-CONH₂_800 based capacitor, the values of retention of capacitance are higher than the heat treated at 500 °C due to the generation of surface functionalities with higher electrochemical stability at this temperature (pyrroles/pyridones). However, the performance is still poorer than that found for the capacitors based on heat treated carbons at 800 °C (KUA_800 and KUA-N_800), since the surface reactivity of this heat treated carbon material is higher than the found in the related materials.

These results point out that heat treatments improve the performance of carbon electrodes upon durability mostly due to the removal of detrimental oxygen functionalities. However, the performance is further improved when the doping strategies are carried out by wet methods at low temperature. KUA-N and KUA-CONH₂ show better performance than the related heat-treated samples not only in terms of retention of capacitance but also in the increase of resistance. Indeed, the supercapacitors constructed from both N-doped carbons show the lowest increase of resistance of the whole series. This is a consequence of combining the beneficial effect of the decrease in the most reactive oxygen groups with the production of nitrogen functional groups with remarkable stabilizing effect, especially in the case of amide-like functionalities. Also, the generation of reactive sites during the thermal treatment is avoided under these mild conditions. Thus, the nitrogen doping method at mild conditions is a promising strategy to improve the performance of any carbon material as electrode for supercapacitors.

As a proof of concept, a commercial activated carbon used for supercapacitor application was successfully functionalized with nitrogen and tested for durability in organic electrolyte (see Supplementary Data II, Figures S4–S6, Table S1). After the durability test, an increase of retention of capacitance of 7% was determined, confirming the viability of this methodology to improve the electrochemical stability of carbon materials.

4. Conclusions

Activated carbons with a similar porosity but different surface chemistry have been prepared by combining chemical functionalization methods at mild conditions and post-thermal treatments. The doping methods at low temperature provide the incorporation of ~4% at. of N in form of different functionalities by consumption of oxygen moieties. The heat treatments diminish the content of heteroatom-containing surface functionalities and produce rearrangements of the nitrogen groups. The surface composition and porosity of the heat-treated samples is almost identical for the whole series of carbons.

The surface chemistry of these carbon materials clearly influences the electrochemical performance when tested as electrodes for the EDLC in organic electrolyte. They show large capacitance values with no significant differences as a consequence of their similar porous texture. The presence of oxygen functional groups affects the rate performance of the capacitor due to the decrease of

conductivity, while nitrogen functional groups (cyclic amides, pyridines, and pyrroles) slightly increase the conductivity of the carbon material.

The effect of surface functionalities upon durability was thoroughly studied. The oxygen functionalities strongly damage the performance of the activated carbons. Thus, the heat treatments of the samples produce an improvement of the electrochemical stability due to the decrease of detrimental oxygen groups. However, the performance is further increased by nitrogen doping at mild conditions, since the treatment combines the positive effect of removing the most reactive oxygen groups with their replacement by nitrogen groups with high electrochemical stability, which is especially beneficial in case of the generation of amide-like functional groups.

Supplementary Materials: The following are available online at <http://www.mdpi.com/2311-5629/6/3/56/s1>, Figure S1. Differential pore size distributions obtained by NL-DFT calculations for all activated carbons; Figure S2. GCD curves obtained for EDLCs (activated carbons-based symmetric capacitors). 1M TEMABF₄/PC. $j = 1000$ mA/g. $V = 2.5$ V; Figure S3. N1s XPS spectrum obtained for YP50F-N activated carbon; Figure S4. N₂ adsorption-desorption isotherms of the activated carbons YP50F and YP50F-N; Figure S5. Cyclic voltammograms in the potential range between 0V and 0.6V for YP50F and YP50F-N electrodes. 1M H₂SO₄. $V = 1$ mV/s; Figure S6. Evolution of capacitance and coulombic efficiency during the durability test for YP50F and YP50F-N based capacitors. 1M TEMABF₄. $j = 40$ mA/g; Table S1. Textural properties and elemental surface composition (XPS and TPD) for YP50F and YP50F-N.

Author Contributions: Conceptualization, D.C.-A., E.M., and S.S.; Formal analysis, M.J.M.-L., R.R.-R., and T.T.; Funding acquisition, D.C.-A., E.M., and S.S.; Investigation, M.J.M.-L., R.R.-R., T.T., Y.H., S.S., E.M., and D.C.-A.; Methodology, M.J.M.-L., R.R.-R., T.T., Y.H., and D.C.-A.; Resources, D.C.-A., E.M., and S.S.; Writing—original draft, M.J.M.-L., R.R.-R., T.T., and Y.H.; Writing—review & editing, D.C.-A., E.M., and S.S. All authors have read and agreed to the published version of the manuscript.

Funding: This research was funded by MINECO, FEDER (CTQ2015-66080-R (MINECO/FEDER), RTI2018-095291-B-I00, ENE2017-90932-REDT, PID2019-105923RB-I00), JSPS KAKENHI (17H03123), and Gunma University Element Functional Science Project. MJML was funded by VALi+d grant (ACIF/2015/374) and mobility grant (BEFPI/2016/006).

Acknowledgments: The authors thank MINECO, FEDER (CTQ2015-66080-R (MINECO/FEDER), RTI2018-095291-B-I00, ENE2017-90932-REDT, PID2019-105923RB-I00), JSPS KAKENHI (17H03123), and Gunma University Element Functional Science Project. MJML acknowledges financial support through VALi+d grant (ACIF/2015/374) and mobility grant (BEFPI/2016/006).

Conflicts of Interest: The authors declare no conflict of interest.

References

1. Conway, B.E. *Electrochemical Supercapacitors: Scientific Fundamentals and Technological Applications*; Springer: New York, NY, USA, 1999.
2. Raza, W.; Ali, F.; Raza, N.; Luo, Y.; Kim, K.-H.; Yang, J.; Kumara, S.; Mehmood, A.; Kwon, E.E. Recent advancements in supercapacitor technology. *Nano Energy* **2018**, *52*, 441–473. [[CrossRef](#)]
3. Béguin, F.; Frackowiak, E. (Eds.) *Carbons for Electrochemical Energy Storage and Conversion Systems*, 1st ed.; CRC Press: Boca Raton, FL, USA, 2009.
4. Le, T.X.H.; Bechelany, M.; Cretin, M. Carbon felt based-electrodes for energy and environmental applications: A review. *Carbon* **2017**, *122*, 564–591. [[CrossRef](#)]
5. Balducci, A. Electrolytes for high voltage electrochemical double layer capacitors: A perspective article. *J. Power Sources* **2016**, *326*, 534–540. [[CrossRef](#)]
6. Béguin, F.; Presser, V.; Balducci, A.; Frackowiak, E. Carbons and Electrolytes for Advanced Supercapacitors. *Adv. Mater.* **2014**, *26*, 2219–2251. [[CrossRef](#)] [[PubMed](#)]
7. Salinas-Torres, D.; Shiraishi, S.; Morallón, E.; Cazorla-Amoros, D. Improvement of carbon materials performance by nitrogen functional groups in electrochemical capacitors in organic electrolyte at severe conditions. *Carbon* **2015**, *82*, 205–213. [[CrossRef](#)]
8. Shiraishi, S. Heat-Treatment and Nitrogen-Doping of Activated Carbons for High Voltage Operation of Electric Double Layer Capacitor. *Key Eng. Mater.* **2011**, *497*, 80–86. [[CrossRef](#)]
9. Mostazo-López, M.J.; Ruiz-Rosas, R.; Morallón, E.; Cazorla-Amoros, D. Nitrogen doped superporous carbon prepared by a mild method. Enhancement of supercapacitor performance. *Int. J. Hydrogen Energy* **2016**, *41*, 19691–19701. [[CrossRef](#)]

10. Frackowiak, E.; Béguin, F. Carbon materials for the electrochemical storage of energy in capacitors. *Carbon* **2001**, *39*, 937–950. [[CrossRef](#)]
11. Paraknowitsch, J.P.; Thomas, A. Doping carbons beyond nitrogen: An overview of advanced heteroatom doped carbons with boron, sulphur and phosphorus for energy applications. *Energy Environ. Sci.* **2013**, *6*, 2839. [[CrossRef](#)]
12. Yang, Z.; Nie, H.; Chen, X.; Chen, X.; Huang, S. Recent progress in doped carbon nanomaterials as effective cathode catalysts for fuel cell oxygen reduction reaction. *J. Power Sources* **2013**, *236*, 238–249. [[CrossRef](#)]
13. Berenguer, R.; Ruiz-Rosas, R.; Gallardo, A.; Cazorla-Amoros, D.; Morallón, E.; Nishihara, H.; Kyotani, T.; Rodríguez-Mirasol, J.; Cordero, T. Enhanced electro-oxidation resistance of carbon electrodes induced by phosphorus surface groups. *Carbon* **2015**, *95*, 681–689. [[CrossRef](#)]
14. González-Gaitán, C.; Ruiz-Rosas, R.; Nishihara, H.; Kyotani, T.; Morallón, E.; Cazorla-Amoros, D. Successful functionalization of superporous zeolite templated carbon using aminobenzene acids and electrochemical methods. *Carbon* **2016**, *99*, 157–166. [[CrossRef](#)]
15. Ornelas, O.; Sieben, J.M.; Ruiz-Rosas, R.; Morallón, E.; Cazorla-Amoros, D.; Geng, J.; Soin, N.; Siores, E.; Johnson, B.F.G. On the origin of the high capacitance of nitrogen-containing carbon nanotubes in acidic and alkaline electrolytes. *Chem. Commun.* **2014**, *50*, 11343–11346. [[CrossRef](#)] [[PubMed](#)]
16. Le, T.-X.-H.; Esmilaire, R.; Drobek, M.; Bechelany, M.; Vallicari, C.; Cerneaux, S.; Julbe, A.; Cretin, M. Nitrogen-Doped Graphitized Carbon Electrodes for Biorefractory Pollutant Removal. *J. Phys. Chem. C* **2017**, *121*, 15188–15197. [[CrossRef](#)]
17. Mostazo-López, M.J.; Ruiz-Rosas, R.; Castro-Muñiz, A.; Nishihara, H.; Kyotani, T.; Morallón, E.; Cazorla-Amoros, D. Ultraporous nitrogen-doped zeolite-templated carbon for high power density aqueous-based supercapacitors. *Carbon* **2018**, *129*, 510–519. [[CrossRef](#)]
18. Hulicova-Jurcakova, D.; Kodama, M.; Shiraiishi, S.; Hatori, H.; Zhu, Z.; Lu, G. Nitrogen-Enriched Nonporous Carbon Electrodes with Extraordinary Supercapacitance. *Adv. Funct. Mater.* **2009**, *19*, 1800–1809. [[CrossRef](#)]
19. Candelaria, S.L.; Garcia, B.B.; Liu, D.; Cao, G. Nitrogen modification of highly porous carbon for improved supercapacitor performance. *J. Mater. Chem.* **2012**, *22*, 9884. [[CrossRef](#)]
20. Kawaguchi, M.; Yamanaka, T.; Hayashi, Y.; Oda, H. Preparation and Capacitive Properties of a Carbonaceous Material Containing Nitrogen. *J. Electrochem. Soc.* **2010**, *157*, A35. [[CrossRef](#)]
21. Cazorla-Amoros, D.; Lozano-Castelló, D.; Morallón, E.; Bleda-Martínez, M.J.; Linares-Solano, A.; Shiraiishi, S. Measuring cycle efficiency and capacitance of chemically activated carbons in propylene carbonate. *Carbon* **2010**, *48*, 1451–1456. [[CrossRef](#)]
22. Raymundo-Piñero, E.; Kierzek, K.; Machnikowski, J.; Béguin, F. Relationship between the nanoporous texture of activated carbons and their capacitance properties in different electrolytes. *Carbon* **2006**, *44*, 2498–2507. [[CrossRef](#)]
23. Shen, W.; Fan, W. Nitrogen-containing porous carbons: Synthesis and application. *J. Mater. Chem. A* **2013**, *1*, 999–1013. [[CrossRef](#)]
24. Deng, Y.; Zou, K.; Xie, Y.; Ji, X. Review on recent advances in nitrogen-doped carbons: Preparations and applications in supercapacitors. *J. Mater. Chem. A* **2016**, *4*, 1144–1173. [[CrossRef](#)]
25. Raymundo-Piñero, E.; Cazorla-Amoros, D.; Linares-Solano, A. The role of different nitrogen functional groups on the removal of SO₂ from flue gases by N-doped activated carbon powders and fibres. *Carbon* **2003**, *41*, 1925–1932. [[CrossRef](#)]
26. Itoi, H.; Nishihara, H.; Kyotani, T. Effect of Heteroatoms in Ordered Microporous Carbons on Their Electrochemical Capacitance. *Langmuir* **2016**, *32*, 11997–12004. [[CrossRef](#)]
27. Nishihara, H.; Hou, P.-X.; Li, L.-X.; Ito, M.; Uchiyama, M.; Kaburagi, T.; Ikura, A.; Katamura, J.; Kawarada, T.; Mizuuchi, K.; et al. High-Pressure Hydrogen Storage in Zeolite-Templated Carbon. *J. Phys. Chem. C* **2009**, *113*, 3189–3196. [[CrossRef](#)]
28. Mostazo-López, M.J.; Ruiz-Rosas, R.; Morallón, E.; Cazorla-Amoros, D. Generation of nitrogen functionalities on activated carbons by amidation reactions and Hofmann rearrangement: Chemical and electrochemical characterization. *Carbon* **2015**, *91*, 252–265. [[CrossRef](#)]
29. Tagaya, T.; Hatakeyama, Y.; Shiraiishi, S.; Tsukada, H.; Mostazo-López, M.J.; Morallón, E.; Cazorla-Amorós, D. Nitrogen-Doped Seamless Activated Carbon Electrode with Excellent Durability for Electric Double Layer Capacitor. *J. Electrochem. Soc.* **2020**, *167*, 060523. [[CrossRef](#)]

30. Lozano-Castelló, D.; Lillo-Ródenas, M.A.; Cazorla-Amoros, D.; Linares-Solano, A. Preparation of activated carbons from Spanish anthracite. *Carbon* **2001**, *39*, 741–749. [[CrossRef](#)]
31. Cazorla-Amoros, D.; Alcañiz-Monge, J.; de La de La Casa-Lillo, M.A.; Linares-Solano, A. CO₂ Adsorptive to Characterize Carbon Molecular Sieves and Activated Carbons. *Langmuir* **1998**, *14*, 4589–4596. [[CrossRef](#)]
32. Lozano-Castelló, D.; Cazorla-Amoros, D.; Linares-Solano, A.; Shiraishi, S.; Kurihara, H.; Oya, A. Influence of pore structure and surface chemistry on electric double layer capacitance in non-aqueous electrolyte. *Carbon* **2003**, *41*, 1765–1775. [[CrossRef](#)]
33. Bleda-Martínez, M.; Lozano-Castelló, D.; Morallón, E.; Cazorla-Amoros, D.; Linares-Solano, A. Chemical and electrochemical characterization of porous carbon materials. *Carbon* **2006**, *44*, 2642–2651. [[CrossRef](#)]
34. Raymundo-Piñero, E.; Cazorla-Amoros, D.; Linares-Solano, A.; Find, J.; Wild, U.; Schlögl, R. Structural characterization of N-containing activated carbon fibers prepared from a low softening point petroleum pitch and a melamine resin. *Carbon* **2002**, *40*, 597–608. [[CrossRef](#)]
35. Jansen, R.; van Bekkum, H. XPS of nitrogen-containing functional groups on activated carbon. *Carbon* **1995**, *33*, 1021–1027. [[CrossRef](#)]
36. Yamada, Y.; Kim, J.; Matsuo, S.; Sato, S. Nitrogen-containing graphene analyzed by X-ray photoelectron spectroscopy. *Carbon* **2014**, *70*, 59–74. [[CrossRef](#)]
37. Figueiredo, J.; Pereira, M.F.R.; Freitas, M.M.; Órfão, J.J.D.M. Modification of the surface chemistry of activated carbons. *Carbon* **1999**, *37*, 1379–1389. [[CrossRef](#)]
38. Arrigo, R.; Hävecker, M.; Wrabetz, S.; Blume, R.; Lerch, M.; McGregor, J.; Parrott, E.P.J.; Zeitler, J.A.; Gladden, L.; Knop-Gericke, A.; et al. Tuning the Acid/Base Properties of Nanocarbons by Functionalization via Amination. *J. Am. Chem. Soc.* **2010**, *132*, 9616–9630. [[CrossRef](#)]
39. Strelko, V.V.; Kuts, V.S.; Thrower, P.A. On the mechanism of possible influence of heteroatoms of nitrogen, boron and phosphorus in a carbon matrix on the catalytic activity of carbons in electron transfer reactions. *Carbon* **2000**, *38*, 1499–1503. [[CrossRef](#)]
40. Shiraishi, S. Electrochemical Performance. In *Materials Science and Engineering of Carbon*; Inagaki, M., Ed.; Tsinghua University Press Limited: Beijing, China; Elsevier Inc.: Amsterdam, The Netherlands, 2016; pp. 205–226.
41. Weingarth, D.; Noh, H.; Foelske, A.; Wokaun, A.; Kötz, R. A reliable determination method of stability limits for electrochemical double layer capacitors. *Electrochim. Acta* **2013**, *103*, 119–124. [[CrossRef](#)]
42. Weingarth, D.; Foelske, A.; Kötz, R. Cycle versus voltage hold—Which is the better stability test for electrochemical double layer capacitors? *J. Power Sources* **2013**, *225*, 84–88. [[CrossRef](#)]
43. Ruch, P.W.; Cericola, D.; Foelske-Schmitz, A.; Kotz, R.; Wokaun, A. Aging of electrochemical double layer capacitors with acetonitrile-based electrolyte at elevated voltages. *Electrochim. Acta* **2010**, *55*, 4412–4420. [[CrossRef](#)]
44. Ratajczak, P.; Jurewicz, K.; Béguin, F. Factors contributing to ageing of high voltage carbon/carbon supercapacitors in salt aqueous electrolyte. *J. Appl. Electrochem.* **2013**, *44*, 475–480. [[CrossRef](#)]
45. Kotz, R.; Hahn, M.; Gallay, R. Temperature behavior and impedance fundamentals of supercapacitors. *J. Power Sources* **2006**, *154*, 550–555. [[CrossRef](#)]
46. Bohlen, O.; Kowal, J.; Sauer, D.U. Ageing behaviour of electrochemical double layer capacitors. *J. Power Sources* **2007**, *172*, 468–475. [[CrossRef](#)]

